


Defect Line Coarsening and Refinement in Active Nematics

Nika Kralj¹, Miha Ravnik^{1,2} and Žiga Kos^{1,2,3,*}

¹*Faculty of Mathematics and Physics, University of Ljubljana, Jadranska 19, 1000 Ljubljana, Slovenia*

²*Condensed Matter Physics Department, J. Stefan Institute, Jamova 39, 1000 Ljubljana, Slovenia*

³*International Institute for Sustainability with Knotted Chiral Meta Matter, Hiroshima University, Higashihiroshima 739-8511, Japan*

 (Received 22 April 2022; revised 9 February 2023; accepted 15 February 2023; published 21 March 2023)

Active matter is naturally out of equilibrium which results in the emergence of diverse dynamic steady states, including the omnipresent chaotic state known as the active turbulence. However, much less is known how active systems dynamically depart out of these configurations, such as get excited or damped to a different dynamic steady state. In this Letter, we demonstrate the coarsening and refinement dynamics of topological defect lines in three-dimensional active nematic turbulence. Specifically, using theory and numerical modeling, we are able to predict the evolution of the active defect density away from the steady state due to time-dependent activity or viscoelastic material properties, establishing a single length scale phenomenological description of defect line coarsening and refinement in a three-dimensional active nematic. The approach is first applied to growth dynamics of a single active defect loop, and then to a full three-dimensional active defect network. More generally, this Letter provides insight into the general coarsening phenomena between dynamical regimes in 3D active matter, with a possible analogy in other physical systems.

DOI: [10.1103/PhysRevLett.130.128101](https://doi.org/10.1103/PhysRevLett.130.128101)

Active matter systems are distinctly nonequilibrium in nature, but regularly form diverse dynamic steady states [1,2]. Much like passive systems that evolve over time to reach equilibrium upon a stimulus, active systems can evolve into new or different dynamic steady states and coarsening is observed as the major transitional mechanism [3–7]. Density correlation functions during coarsening separate active suspensions into classes [8] with structure functions commonly deviating from the Porod’s law that is generally expected for systems relaxing toward equilibrium [8]. In active binary fluids, the initial length scale dynamics during coarsening is reported to follow the same time dependence as for passive fluids [9,10], while at larger scales activity takes over and eventually a dynamic steady state is established [9]. Coarsening was observed also in two-dimensional dry active nematics and is based on annihilation of half-integer defect pairs [11].

Active nematics are a class of active materials, which exhibit apolar orientational order along the director \mathbf{n} , with material examples including microtubule mixtures and bacterial suspensions [2,12–15]. In three dimensions, bulk active nematics form the dynamic steady state called active turbulence, which at the structural level is a dynamic rewiring network of defect lines and loops [16–18], driven by the anisotropic active stress [19,20]. Recently, it was

shown that advective terms are suppressed in active fluids [21,22] and in the steady state the energy injection is exactly matched by the viscous dissipation at each scale [22]. Defect line segments are driven by the self-propulsion velocity depending on their local director profile, leading the defect loops to grow, shrink, and buckle in time [23,24].

Beyond the active matter, the phase ordering kinetics through coarsening exhibits universal behavior across a range of physical systems, as underlain with the fundamental role of the topological defects within the order parameter field [25]. Universal rules for phase kinetics are typically obtained through energetic arguments [25], which opens a question of what novel insights active matter energetics as an emergent field can provide. Notably, the universal of defects in the shape of lines and loops—first described by Kibble for cosmic strings [26] and later predicted by Zurek for superfluid helium [27]—was experimentally observed in (passive, i.e., not active) nematic liquid crystals [28].

In this Letter, we show transitional dynamics from initial configurations toward a dynamic steady state and also between dynamic steady states of 3D active nematic turbulence, as distinctly determined by the coarsening and refinement of a network of topological defect lines and loops. We construct an analytical model of the collapse or growth of a single defect loop and then generalize it to the coarsening and refinement of the full 3D defect network. The approach provides analytic insight into the effective phase ordering kinetics toward dynamic steady states, as triggered by changes in the main material parameters, such as activity or even nematic elasticity and viscosity. While the notion of self-propelled defects is unique for active

Published by the American Physical Society under the terms of the Creative Commons Attribution 4.0 International license. Further distribution of this work must maintain attribution to the author(s) and the published article’s title, journal citation, and DOI.

nematics, the demonstrated coarsening and refinement indicates possible universal behavior applicable to different physical systems, including cosmic string dynamics.

Active nematics are described by the experimentally supported [16,29] mesoscopic active nematodynamic formulation [30,31]. The approach is based on the coupled dynamics of the two main fields—the velocity field \mathbf{v} and the nematic order parameter tensor \mathbf{Q} with the director \mathbf{n} as the main eigenvector. The flow field is determined by the active propulsion due to the active stress that is proportional to \mathbf{Q} [19], and by the viscous coupling to the nematic order, whereas the dynamics of \mathbf{Q} is determined by the interplay between the dissipative relaxation toward the equilibrium and coupling to the material flow (Supplemental Material [32]). We solve this model by using a hybrid lattice Boltzmann algorithm with the results given in units of mesh resolution Δx , tensorial elastic constant L , and rotational viscosity Γ . Such a numerical approach was shown to reproduce different structural and dynamical features of multiple experimental two-dimensional [33,34] and three-dimensional active nematic systems [16,18,23].

Coarsening of a defect network of three-dimensional active turbulence is demonstrated in Fig. 1, following a quench from a high defect density regime. The coarsening dynamics shows gradually decreasing defect density, and notably includes both shrinkage *and* expansion of the length of topological defect loops (Fig. 1). We elucidate such shrinking and expansion dynamics by first considering the kinetics of isolated active defect loops that can be captured as the competition between the (elastic) line tension and the active propulsion. For an in-plane zero-topological charge loop of radius r as shown in Fig. 2(a), the defect line tension can be estimated as

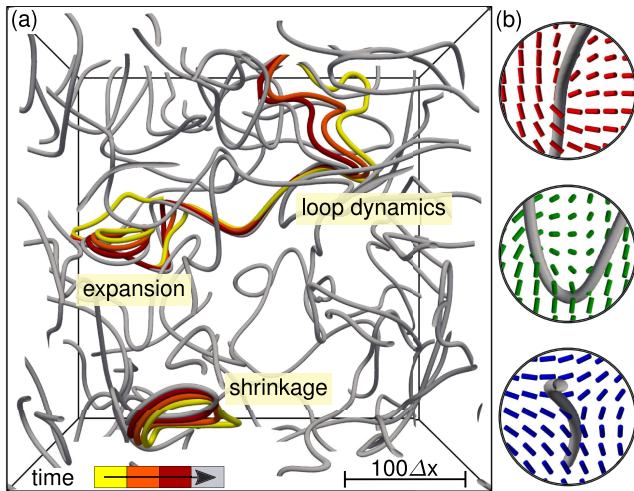


FIG. 1. Coarsening dynamics of active nematic turbulence. (a) A snapshot of a defect line network (gray) during coarsening process. Additionally, selected defect line segments are drawn in different colors at earlier time intervals $50\Delta x^2/(\Gamma L)$ apart. (b) The director field rotates for an angle of π around the defect lines: from $+1/2$ profiles (red), to twist (green) and $-1/2$ profiles (blue).

$T = (\pi K/4) \ln(r/r_{\min})$, where K is the single elastic constant proportional to tensorial elastic constant L (see Supplemental Material [32]), and r_{\min} is the defect core size [35,36]. Such a defect line also experiences an effective drag force due to local rotations of the director field as it moves through the material and can be estimated as $f_{\text{drag}} = c_{\text{drag}} v = (\pi/4)\gamma_1 v \ln(r/r_{\min})$, where c_{drag} is the drag coefficient, γ_1 the rotational viscosity, and v its velocity with respect to the flow of the nematic fluid [35]. The active self-propulsion flow velocity v_0 depends on the director field of different defect loop segments [23,37] and varies from $v_0 \approx 0$ for the $-1/2$ section to $v_0 \approx |\alpha|r/4\eta$ for the $+1/2$ defect loop section. If assuming a circular loop, all these contributions give a dynamical equation for the active nematic defect loop radius

$$\dot{r} = \frac{v_0}{2} - \frac{T}{c_{\text{drag}} r} = \frac{|\alpha|r}{8\eta} - \frac{K}{\gamma_1 r}. \quad (1)$$

Solving Eq. (1) gives the time dependence of loop radius

$$r(t) = r_c \left[1 + \left(\frac{r_0^2}{r_c^2} - 1 \right) e^{t/\tau_{\text{loop}}} \right]^{1/2}, \quad (2)$$

where $\tau_{\text{loop}} = 4\eta/|\alpha|$ is the characteristic timescale of isolated defect loops, r_0 is the initial loop radius at $t = 0$, and $r_c = \sqrt{(8\eta K)/(\gamma_1 |\alpha|)}$ is the critical radius for which the active propulsion exactly counterbalances the loop line tension (i.e., $\dot{r} = 0$). r_c is explicitly dependent on nematic elasticity, activity, and rotational viscosity, which provides a direct analytic insight into possible control of active defect loop kinetics; for $r > r_c$ the loops expand, whereas for $r < r_c$ the loops shrink. Note that the existence of a critical radius has analogies with the spontaneous flow transitions in polar gels [20], but with a notable difference that in polar gels the transition is symmetry breaking, whereas for active loops the flow is always generated and competes with the elasticity-induced shrinking.

The analytical model is compared to the full numerical simulation, observing excellent agreement (Fig. 2). A loop with a fixed initial radius is let to dynamically evolve at different activities and depending on the activity, this leads to shrinking (Supplemental Material [32], Movie 1) or expanding (Movie 2) dynamics. A fit of Eq. (2) to the simulation data gives $1/\tau_{\text{loop}} = 0.186\Gamma\alpha$ and $r_c^2/\tau_{\text{loop}} = 2.78\Gamma L$, which compares well to values of $1/\tau_{\text{loop}} = 0.182\Gamma\alpha$ and $r_c^2/\tau_{\text{loop}} = 2\Gamma L$ that are calculated directly from the viscoelastic parameters of the simulation. More generally, now supported also by the numerical simulations, we show that the nematic elasticity, active propulsion, and the viscous drag are the main mechanisms of the three-dimensional active defect kinetics.

The mechanisms of defect line tension, drag force, and self-propulsion that were used to describe the single active defects can be generalized to the overall coarsening dynamics of a full three-dimensional active defect network.

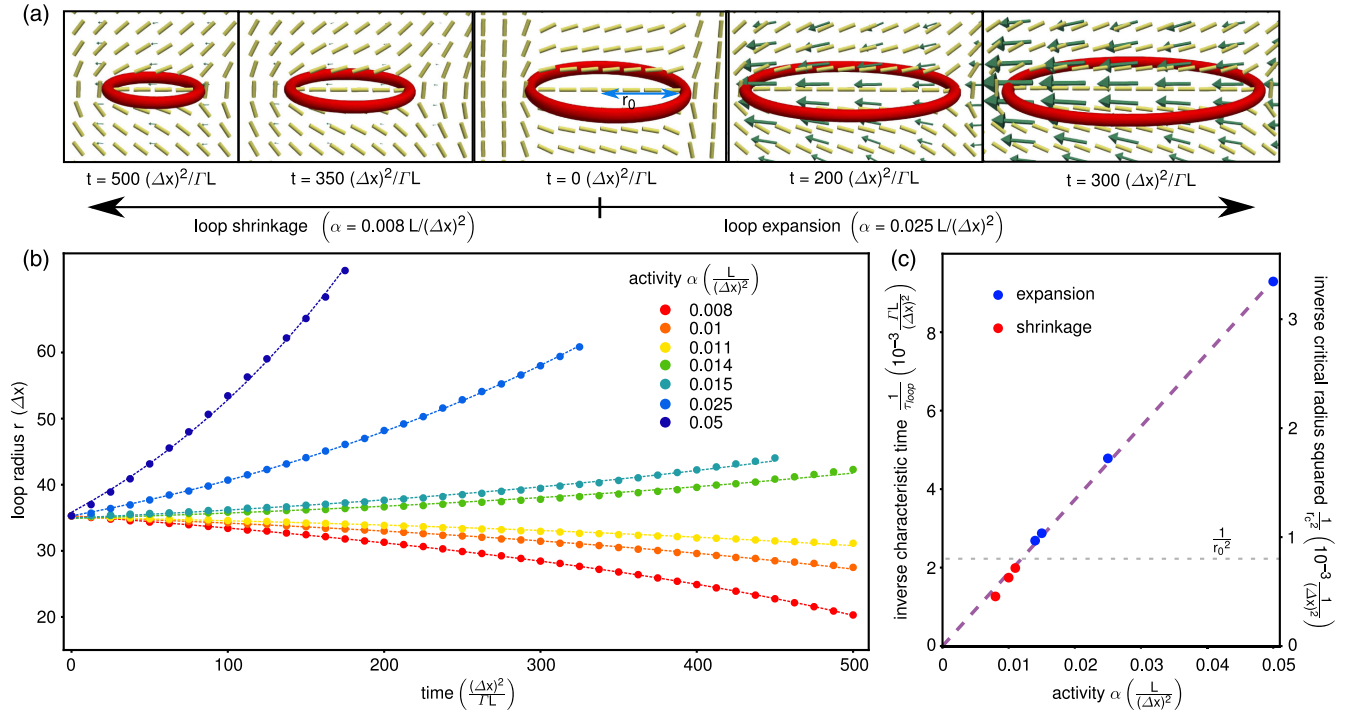


FIG. 2. Shrinking and expanding dynamics of isolated active nematic defect loop. (a) Depending on activity α , the defect loop either shrinks or expands in time; the panels show the defect loop as isosurface of degree of order (red), director field (yellow rods), and velocity field (green arrows). The defect loop has $+1/2$ profile at the left side, and $-1/2$ profile on the right side, which generates an overall self-propulsion velocity and a local active stress on the loop toward the left. (b) Single loop radius as function of time for different activities. Radius is determined as the loop left-to-right dimension in panel (a). The dashed line is a fit [Eq. (2)] to the numerical data with fit parameters τ_{loop} and activity-independent parameter r_c^2/τ_{loop} , obtaining $r_c^2/\tau_{\text{loop}} = 2.78\Gamma L$. (c) Critical radius r_c and initial radius $r_0 = 35.3\Delta x$ determine shrinkage ($r_0 < r_c$) and expansion ($r_0 > r_c$) regimes. A linear dependence of $1/\tau_{\text{loop}}$ (or equally $1/r_c^2$) on activity is obtained with the slope of $1/\tau_{\text{loop}} = 0.186\Gamma\alpha$.

Our model is based on a single time-dependent length scale ξ , which represents both typical radius of curvature and typical separation of defect lines [28,35]. Notice that during active coarsening, both the average defect-defect separation and the curvature decrease over time [Figs. 3(a) and 3(b)]. Specifically, ξ is calculated as $\rho = 1/\xi^2$ where ρ is the total defect length over unit volume. The coarsening dynamics of the defect networks is now described as the time evolution of the single length scale ξ based on a balance between the defect line tension T/ξ and viscous drag $\Gamma(\dot{\xi} + bv_0)$, where the phenomenological parameter b describes the effective self-propulsion velocity of defect lines. Generalized from a single defect loop [Eq. (1)] to a defect network, here the line tension straightens and spaces out the defects in time, which gives the main dynamic equation of active coarsening

$$\dot{\xi} = a \frac{K}{\gamma_1 \xi} - b \frac{|\alpha| \xi}{4\eta}, \quad (3)$$

where in analogy to the passive coarsening [38,39], we use dimensionless parameter a to describe the relative strength of line tension compared to drag force in a defect

network. Equation (3) can be rewritten in terms of the defect density

$$\dot{\rho} = \frac{b|\alpha|}{2\eta} \rho - \frac{2aK}{\gamma_1} \rho^2, \quad (4)$$

and upon integration at constant activity, the coarsening equation for the active defect density is obtained

$$\rho(t) = \rho_c \left[1 + \left(\frac{\rho_0}{\rho_c} - 1 \right) e^{-t/\tau} \right]^{-1}, \quad (5)$$

where $\tau = (2\eta)/(b|\alpha|)$, $\rho_c = (b|\alpha|\gamma_1)/(4\eta aK)$, and ρ_0 is the initial density at $t = 0$. Equation (5) shows how the defect density evolves from an initial value of ρ_0 toward a dynamic steady state ρ_c with a well-defined timescale τ .

Numerical modeling of coarsening for a full active nematodynamic approach is shown in Fig. 3 and Supplemental Material [32], Movie 3. The simulations are performed from an initial configuration of a random director field at each data point and at $t \approx 10\Delta x^2/(\Gamma L)$ a dense defect network is formed, which coarsens over time [Fig. 3(c) and Supplemental Material, Fig. S1]. For high

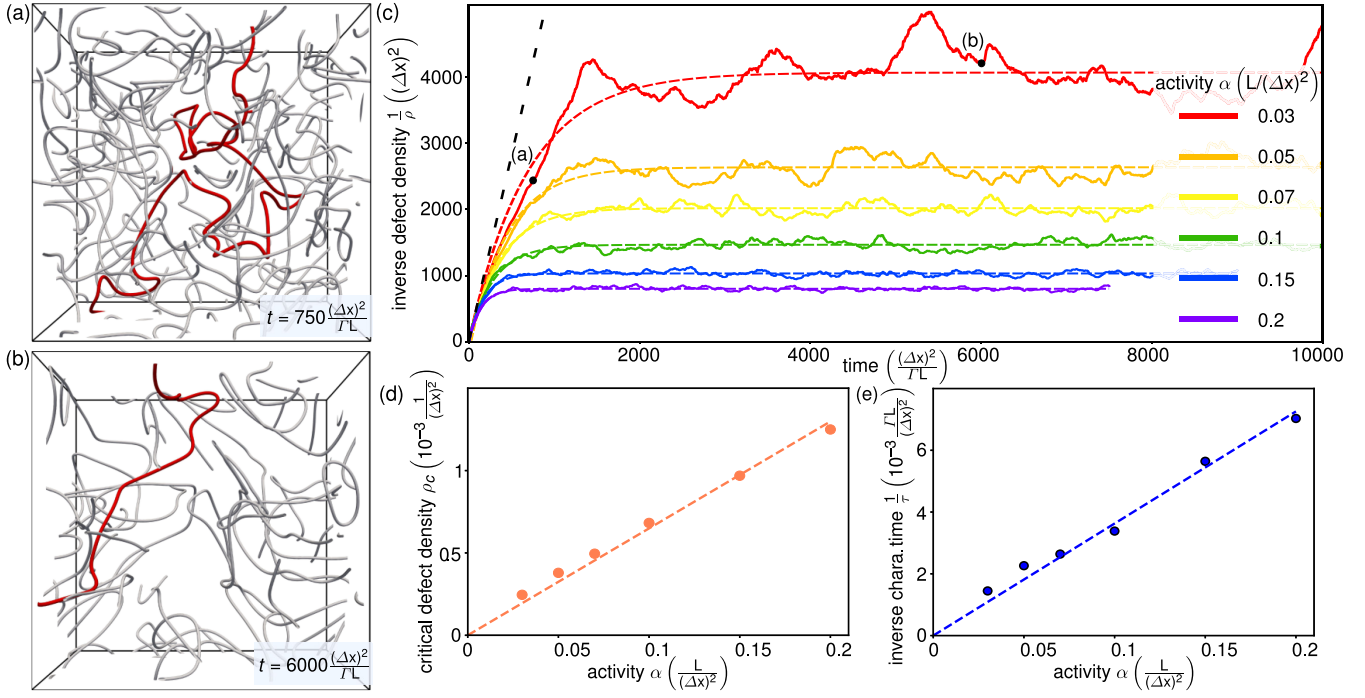


FIG. 3. Coarsening dynamics of 3D active nematic turbulence. (a) Defect network at short time in the coarsening dynamics. A selected connected defect segment is colored in red. (b) Defect network at later time in the coarsening dynamics. Defect line segments are further apart and show smaller curvature compared to (a). (c) Inverse defect density over time for different activities. Dashed lines are fits to Eq. (5) to the simulation data. Black dashed line represents the activity-independent initial density dynamics. The fluctuations of the defect density at later times is the effect of the finite simulation volume but with a well determined average. (d) Steady-state defect density as dependent on activity; linear fit (dashed line) has the slope of $0.0065/L$. (e) Linear dependence of the inverse characteristic time on activity; the linear fit has coefficient of 0.036Γ . Points in (d) and (e) are obtained from fits in (c).

defect density at short times after quench, we observe that the coarsening dynamics is independent on activity, which can be explained by the elastic tension being much larger than the active self-propulsion in Eq. (4). At later times, the defect density approaches the steady-state density ρ_c , which we find is linearly proportional to activity [Fig. 3(d)], in full agreement with the analytical model. The rate of approach toward ρ_c is governed by the timescale τ , which is inversely proportional to activity [Fig. 3(e)]. Parameters a and b from the analytical model can now be determined by a linear fit in Figs. 3(d) and 3(e), obtaining $a = 2.8$ and $b = 0.10$. Parameter a is of roughly similar magnitude as in passive (i.e., zero activity) nematics [38], whereas a low value of b indicates that the defects on average are repelled from each other with a much lower velocity than v_0 , which is characteristic for isolated defect loops in Fig. 2. In Supplemental Material [32], we show that the coarsening dynamics is not significantly altered even for simulations with multiple nematic elastic constants (Fig. S5).

Active refinement is—oppositely to coarsening—characterized by the proliferation of defects (for example, induced by an increase of activity) and it occurs in the regime where active propulsion prevails over the line tension. Figure 4 and Supplemental Material [32], Movie 4 show the defect density upon active refinement from a full

numerical simulation and in agreement with the theoretical model [Eq. (4)]. Figure 4 also shows that the rate of the activity change affects the refinement dynamics, as it has to be compared to the characteristic time $\tau(t)$. Fast changes in activity (red line in Fig. 4) can be described by constant activity dynamics [Eq. (5)], whereas for other regimes (blue and green lines in Fig. 4) the full time-dependent activity $\alpha(t)$ has to be considered in Eq. (4). More generally, the results show that the introduced approach also well covers the *time-dependent* changes in the active nematic material parameters, such as activity, elasticity, and viscosity, indicating an exciting analytic insight into the kinetics of active states out of the dynamic equilibrium. Refinement could also be considered during a transition from an aligned initial condition to a defect network. We show such an example in Fig. S4.

Experimentally, the demonstrated active coarsening (or refinement) could be induced by (meso)phase transitions into a nematic phase, triggered by a pressure or temperature quench [28,40], or possibly even by changing the activity as the nematic material parameters are known to be activity dependent [41,42]. The transition could be studied also in view of the Kibble-Zurek mechanism, which is known to describe structure formation in liquid crystals [43,44], and could interestingly be additionally coupled to curved interfaces [45] and topology of the confining space [46].

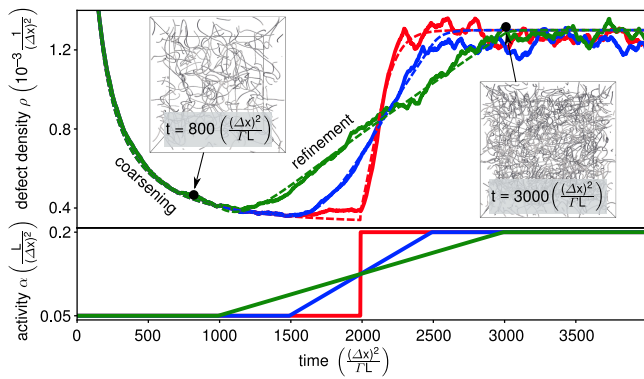


FIG. 4. Active refinement induced by time-varying activity. Defect density (top graph) is shown for the three different time-varying activities (bottom graph). Note the matching colors. The dynamics is initiated at $t = 0$ from a random director field, leading first to coarsening which upon an activity increase changes to refinement. Dashed lines are fits with Eq. (4).

The demonstrated coarsening and refinement of active defects also shows interesting implications beyond soft and active matter. Distinctly, at zero activity, the coarsening dynamics of nematic defect strings is known to share strong mathematical similarities with cosmic strings and condensed matter systems [26,27], whereas here we show that activity can contribute new coarsening terms. Namely, in an active nematic system, the time derivative of the characteristic length scale ξ [Eq. (3)] equals an elastic term proportional to $1/\xi$ and an active term proportional to ξ . This coarsening dynamics shows an interesting analogy with the velocity-dependent one-scale cosmic string model [47,48], where (i) the friction term due to particle scattering proportional to $1/\xi$ is known to give the Kibble coarsening scaling $\xi \sim t^{0.5}$, and (ii) the term proportional to $H\xi$, where H is the Hubble parameter, accounts for the expansion of the Universe. Both terms in the cosmic string model are positive and promote the coarsening dynamics, whereas for active nematics the ξ term is negative ($\dot{\xi} \sim -\xi$) and as we demonstrate can slow down the coarsening and leads to a dynamic steady state with a finite defect density. Such a term would correspond to coarsening of a string network in a shrinking universe. More generally, this analogy provides novel unprecedented parallels between active matter and cosmology.

The authors acknowledge funding from Slovenian Research Agency (ARRS) under Contracts P1-0099, N1-0124, J1-1697, J1-2462, N1-0195, and from European Research Council Grant LOGOS.

* ziga.kos@fmf.uni-lj.si

[1] G. Gompper, R. G. Winkler, T. Speck, A. Solon, C. Nardini, F. Peruani, H. Löwen, R. Golestanian, U. B. Kaupp, L. Alvarez *et al.*, *J. Phys. Condens. Matter* **32**, 193001 (2020).

[2] M. C. Marchetti, J. F. Joanny, S. Ramaswamy, T. B. Liverpool, J. Prost, M. Rao, and R. A. Simha, *Rev. Mod. Phys.* **85**, 1143 (2013).

[3] D. Geyer, D. Martin, J. Tailleur, and D. Bartolo, *Phys. Rev. X* **9**, 031043 (2019).

[4] G. S. Redner, M. F. Hagan, and A. Baskaran, *Phys. Rev. Lett.* **110**, 055701 (2013).

[5] F. Fadda, D. A. Matoz-Fernandez, R. van Roij, and S. Jabbari-Farouji, *arXiv:2203.05213*.

[6] S. Chakraborty and S. K. Das, *J. Chem. Phys.* **153**, 044905 (2020).

[7] G. Gonnella, D. Marenduzzo, A. Suma, and A. Tiribocchi, *C. R. Phys.* **16**, 316 (2015).

[8] S. Dey, D. Das, and R. Rajesh, *Phys. Rev. Lett.* **108**, 238001 (2012).

[9] S. Berti, G. Boffetta, M. Cencini, and A. Vulpiani, *Phys. Rev. Lett.* **95**, 224501 (2005).

[10] S. Sabrina, M. Spellings, S. C. Glotzer, and K. J. M. Bishop, *Soft Matter* **11**, 8409 (2015).

[11] S. Mishra, S. Puri, and S. Ramaswamy, *Phil. Trans. R. Soc. A* **372**, 20130364 (2014).

[12] T. Sanchez, D. T. N. Chen, S. J. DeCamp, M. Heymann, and Z. Dogic, *Nature (London)* **491**, 431 (2012).

[13] H. H. Wensink, J. Dunkel, S. Heidenreich, K. Drescher, R. E. Goldstein, H. Lowen, and J. M. Yeomans, *Proc. Natl. Acad. Sci. U.S.A.* **109**, 14308 (2012).

[14] R. Alert, J. Casademunt, and J.-F. Joanny, *Annu. Rev. Condens. Matter Phys.* **13**, 143 (2022).

[15] J. Hardouin, J. Laurent, T. Lopez-Leon, J. Ignés-Mullol, and F. Sagués, *Soft Matter* **16**, 9230 (2020).

[16] G. Duclos, R. Adkins, D. Banerjee, M. S. E. Peterson, M. Varghese, I. Kolvin, A. Baskaran, R. A. Pelcovits, T. R. Powers, A. Baskaran *et al.*, *Science* **367**, 1120 (2020).

[17] J. Urzay, A. Doostmohammadi, and J. M. Yeomans, *J. Fluid Mech.* **822**, 762 (2017).

[18] Ž. Krajncik, Ž. Kos, and M. Ravnik, *Soft Matter* **16**, 9059 (2020).

[19] Y. Hatwalne, S. Ramaswamy, M. Rao, and R. A. Simha, *Phys. Rev. Lett.* **92**, 118101 (2004).

[20] R. Voituriez, J. F. Joanny, and J. Prost, *Europhys. Lett.* **70**, 404 (2005).

[21] L. N. Carenza, L. Biferale, and G. Gonnella, *Europhys. Lett.* **132**, 44003 (2020).

[22] R. Alert, J.-F. Joanny, and J. Casademunt, *Nat. Phys.* **16**, 682 (2020).

[23] J. Binysh, Ž. Kos, S. Čopar, M. Ravnik, and G. P. Alexander, *Phys. Rev. Lett.* **124**, 088001 (2020).

[24] C. Long, X. Tang, R. L. B. Selinger, and J. V. Selinger, *Soft Matter* **17**, 2265 (2021).

[25] A. J. Bray, *Adv. Phys.* **51**, 481 (2010).

[26] T. W. B. Kibble, *J. Phys. A* **9**, 1387 (1976).

[27] W. Zurek, *Phys. Rep.* **276**, 177 (1996).

[28] I. Chuang, R. Durrer, N. Turok, and B. Yurke, *Science* **251**, 1336 (1991).

[29] F. G. Woodhouse and R. E. Goldstein, *Phys. Rev. Lett.* **109**, 168105 (2012).

[30] S. Čopar, J. Aplinc, Ž. Kos, S. Žumer, and M. Ravnik, *Phys. Rev. X* **9**, 031051 (2019).

[31] L. N. Carenza, G. Gonnella, D. Marenduzzo, and G. Negro, *Proc. Natl. Acad. Sci. U.S.A.* **116**, 22065 (2019).

- [32] See Supplemental Material at <http://link.aps.org/supplemental/10.1103/PhysRevLett.130.128101> for an expanded numerical analysis and more details on the analytical model.
- [33] A. Doostmohammadi, J. Ignés-Mullol, J. M. Yeomans, and F. Sagués, *Nat. Commun.* **9**, 045006 (2018).
- [34] R. Zhang, Y. Zhou, M. Rahimi, and J. J. de Pablo, *Nat. Commun.* **7**, 13483 (2016).
- [35] M. Kleman and O. Lavrentovich, *Soft Matter Physics: An Introduction* (Springer, New York, 2003).
- [36] A. Mertelj and M. Čopič, *Phys. Rev. E* **69**, 021711 (2004).
- [37] L. Giomi, M. J. Bowick, P. Mishra, R. Sknepnek, and M. C. Marchetti, *Phil. Trans. R. Soc. A* **372**, 20130365 (2014).
- [38] B. Yurke, A. N. Pargellis, T. Kovacs, and D. Huse, *Phys. Rev. E* **47**, 1525 (1993).
- [39] W. Wang, T. Shiwaku, and T. Hashimoto, *J. Chem. Phys.* **108**, 1618 (1998).
- [40] D. Austin, E. J. Copeland, and T. W. B. Kibble, *Phys. Rev. D* **48**, 5594 (1993).
- [41] S. P. Thampi, A. Doostmohammadi, R. Golestanian, and J. M. Yeomans, *Europhys. Lett.* **112**, 28004 (2015).
- [42] M. E. Cates and J. Tailleur, *Annu. Rev. Condens. Matter Phys.* **6**, 219 (2015).
- [43] Z. Bradač, S. Kralj, and S. Žumer, *J. Chem. Phys.* **135**, 024506 (2011).
- [44] N. Fowler and D. I. Dierking, *ChemPhysChem* **18**, 812 (2017).
- [45] N. Stoop and J. Dunkel, *Soft Matter* **14**, 2329 (2018).
- [46] M. Nikkhou, M. Škarabot, S. Čopar, M. Ravnik, S. Žumer, and I. Muševič, *Nat. Phys.* **11**, 183 (2015).
- [47] C. J. A. P. Martins and E. P. S. Shellard, *Phys. Rev. D* **65**, 043514 (2002).
- [48] C. Martins, I. Rybak, A. Avgoustidis, and E. Shellard, *Phys. Rev. D* **94**, 116017 (2016).